Synthesis, Photophysical, Photochemical, and Computational Studies of Coumarin-Labeled Nicotinamide Derivatives

Pauline Bourbon,[†] Qian Peng,[†] Guillermo Ferraudi,[†,‡] Cynthia Stauffacher,[§] Olaf Wiest,*[,†] and Paul Helquist*[,†]

[†]Department of Chemistry and Biochemistry, University of Notre Dame, 251 Nieuwland Science Hall, Notre Dame, Indiana 46556, United States

[‡]Notre Dame Radiation Research Laboratory, Notre Dame, Indiana 46556, United States

[§]Department of Biological Sciences, Purdue University, 915 West State Street, West Lafayette, Indiana 47907, United States

S *Supporting Information*

ABSTRACT: The syntheses and photophysical/photochemical properties of two amide-tethered coumarin-labeled nicotinamides are described. Photochemical studies of 6-bromo-7-hydroxycoumarin-in-4-ylmethylnicotinamide (BHC-nicotinamide) revealed an unexpected solvent effect. This result is rationalized by computational studies of the different protonation states using TD-DFT with the M06L/6-311+G** method with implicit and explicit solvation models. Molecular orbital energies responsible for the λ_{max} excitation show that the functionalization of the coumarin ring results in a strong red-shift from 330 to 370 nm when the pH of solution is increased from 3.06 to 8.07. From this MO analysis, a model for solvent interactions has been proposed. The BHC-nicotinamide proved to be photochemically stable, which is also interpreted in terms of NBO calculations. The results provide a set of principles for the rational design of either photostable labeling reagents or photolabile cage compounds.
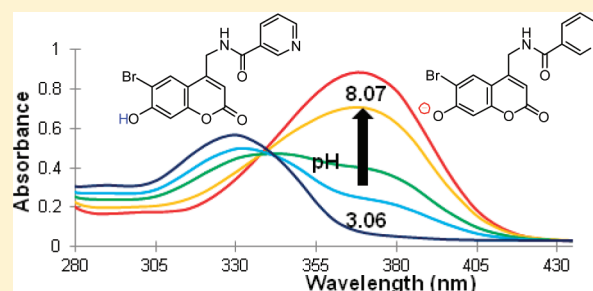
INTRODUCTION

The photochemistry and photophysics of coumarins have been well studied.[1−5] Substitution on the coumarin ring can have drastic effects on its photochemical properties. By changing the substituent on the coumarin ring, one can tune its longest absorption wavelength λ_{max}.[6,7] Substitution at either the 6- or 7-position with electron donating groups or heavy atoms induces a bathochromic shift. For example, conversion of a non-substituted coumarin to the 6-bromo-7-hydroxycoumarin derivative shifts the wavelength from 310 to 370 nm. Furthermore, the effect of the polarity of solvents on the λ_{max} has been subjected to numerous investigations.[8−11] For example, the solvent effect on the absorption spectra of 7-(diethylamino)-, 7-(dimethylamino)-, or 7-amino-4-methyl-2H-chromen-2-one is dependent on the nature of the amino group (Figure 1). In 4-methylumbelliferone, the λ_{max} in acetonitrile is lower than in methanol. However, the reasons for these significant shifts have not been fully understood.
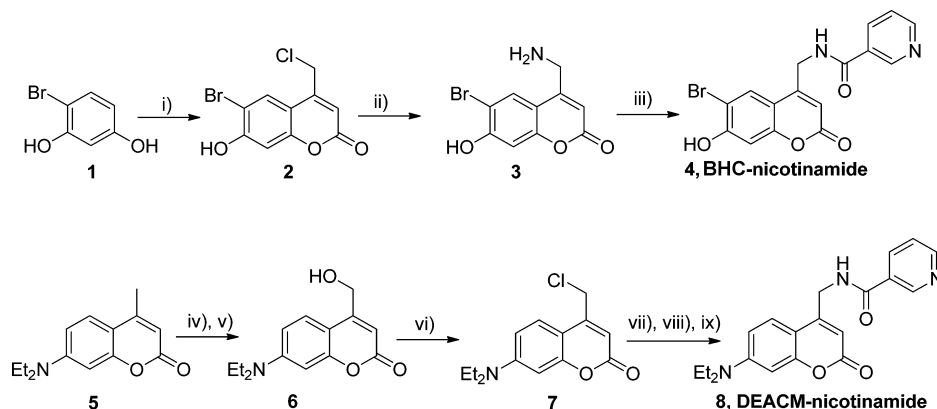
Among the reasons for gaining an understanding of the photobehavior of such compounds has been their application to light activatable cage compounds as a basis for triggering reactions in cells.[12−15] One of the commonly employed photoremovable protecting groups at cellular transparent wavelengths higher than 330 nm is the coumarin moiety. 6-Bromo-7-hydroxycoumarin-4-ylmethyl and 7-(diethylamino)-coumarin-4-ylmethyl are examples that have been used to release an amine as a glutamate,[7] phosphate as RNA,[16] diols,[17] carboxylic acids[18] and alcohols.[19]

The bulk of these previous photochemical and photophysical studies have focused on compounds having C−O bonds such as ester derivatives as the sites of reactions of interest, whereas corresponding C−N derivatives such as amides have not received comparable attention. We have therefore begun a study of nicotinamide linked by amide-based C−N bonds to different coumarins. The choice of nicotinamide in this study has been selected as a model substrate for NAD⁺. In comparison with the photocleavable esters, the amides may be expected to be more stable and may therefore function as useful photolabeled derivatives for cellular studies of NAD⁺-dependent enzymatic reactions. In particular, we have begun these studies with an investigation of the effects of pH and

Figure 1. Structure of different coumarin.

7-amino-4-methyl-2H-chromen-2-one and 4-methylumbelliferone

Scheme 1. Synthesis of Coumarin Derivatives[a]

[a](i) Ethyl 4-chloroacetoacetate, methanesulfonic acid; (ii) NH$_4$OH; (iii) nicotinoyl chloride, DIEA; (iv) SeO$_2$; (v) NaBH$_4$; (vi) pTsCl, py.; (vii) NaN$_3$; (viii) Pd/C, H$_2$; (ix) nicotinoyl chloride, DIEA.
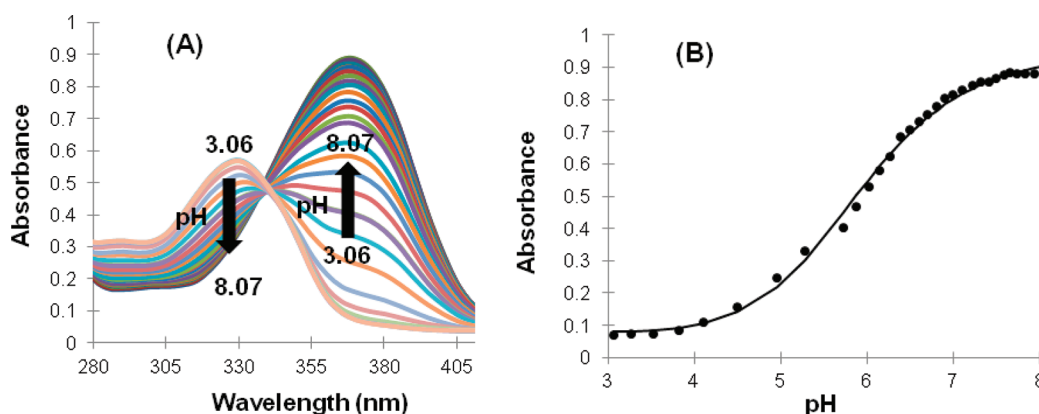

Figure 2. (A) UV−vis spectra of **4** at different pH. (B) pH profile of **4**.

solvent polarity on the photophysics and photochemistry of the newly synthesized 6-bromo-7-hydroxycoumarin-4-ylmethylnicotinamide (BHC-nicotinamide) and N-((7-(diethylamino)-2-oxo-2H-chromen-4-yl)methyl)nicotinamide (DEACM-nicotinamide). We report here the unexpected behavior patterns that were observed for the BHC-nicotinamide, and we provide a rationalization for the experimental observations through use of time dependent density functional theory (TD-DFT) calculations to predict the λ_{max} with the M06L/6-311+G** method using two different implicit solvation models, the conductor-like polarizable continuum model (CPCM) and the more recent SMD model. We also propose a rationalization for the experimentally observed solvent effects using explicit solvent molecules as well as molecular orbital (MO) analysis. Furthermore, with the use of natural bond orbital (NBO) calculations, we are able to propose nicotinamide carbamate derivatives that may be useful compounds for future studies of new photocleavable agents.

■ RESULTS AND DISCUSSION

Synthesis. The labeled BHC-nicotinamide derivative **4** was prepared as shown in Scheme 1 by conversion of the commercially available 4-bromoresorcinol (**1**) to coumarin **2** via a literature procedure in quantitative yield.[18] Conversion to the desired amine **3** was achieved using aqueous ammonium hydroxide in 64% yield. Coupling with nicotinoyl chloride was performed in DMF to give BHC-nicotinamide (**4**) in 58% yield.

The synthesis of the DEACM-nicotinamide, commenced by benzylic oxidation of the commercially available 7-dimethylamino-4-methylcoumarin (**5**) with selenium dioxide, and the resulting aldehyde was reduced to the alcohol **6** in 50% yield.[6] Conversion of the hydroxy derivative to the chloride **7** was effected in 25% yield using p-toluenesulfonyl chloride.[20] Treatment with sodium azide followed by hydrogenation using palladium on carbon furnished the corresponding amine derivative, which was subsequently coupled to nicotinoyl chloride to provided DEACM-nicotinamide (**8**) in 50% yield. In principle, this route could be made much shorter if a reductive amination of the aldehyde derived from the SeO$_2$ oxidation of **5** (step iv) could be effected, but this transformation failed in our hands under several conditions.

Photophysical Characterization. 7-Hydroxy-4-methylcoumarin and 3-carboxy-7-hydroxycoumarin are known to have photophysical properties that are dependent on pH.[21,22] To determine the influence of the pH on the newly synthesized BHC-nicotinamide (**4**), its pH profile was determined in a citrate-phosphate buffer and revealed that the absorption spectrum is strongly dependent on pH (Figure 2A). The protonated phenol form exhibits a λ_{max} at 330 nm and the deprotonated phenolate at 370 nm. From this measurement, the pK_a of BHC-nicotinamide (**4**) was determined to be 5.9 (Figure 2B).

Absorption properties were measured, and extinction coefficients (ε) were calculated according to the Beer−Lambert Law. The λ_{max} of **8** in methanol is 380 nm and has an extinction

coefficient of 24375 $M^{-1} cm^{-1}$. Table 1 and Figure 3 show some unexpected results. Increasing the polarity of the solvent

Table 1. Solvent Effect on 4

solvent	λ_{max}[a]	ε[b]	polarity index P'[c]
Methanol	372	8744	5.1
Acetonitrile	392	11000	5.8
DMSO	408	19491	7.2
pH 3.06[d]	330	8764	10.2
pH 8.07[d]	370	13642	10.2

[a]Maximum absorbance in nm. [b]Extinction coefficient in $M^{-1} cm^{-1}$. [c]Reference 20. [d]Phosphate-citrate buffer.
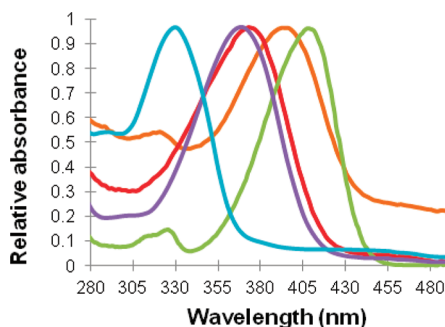

Figure 3. UV−vis spectra of **4** in different solvents. Blue, citrate-phosphate buffer pH = 3.06; purple, citrate-phosphate buffer pH = 8.07, red, methanol; orange, acetonitrile; green, DMSO.

red-shifted the absorption maxima of BHC-nicotinamide (**4**), which can be explained by the stabilization effect of a polar solvent on the excited state. Interestingly, in the presence of a weakly basic buffer, a blue-shift is observed. Normally, we should have expected to observe a bathochromic shift upon increasing the polarity of the solvent.

Understanding the Unexpected UV−Vis λ_{max} in Various Solvents. The results summarized in Table 1 and Figures 2−3 do not provide direct experimental information on the protonation states of BHC-nicotinamide **4**. As shown in Scheme 2, neutral BHC-nicotinamide **4** can either lose one proton from the phenol ring acting as a Brønsted acid to form an anion **4**⁻ or accept a proton on the pyridine ring as a Brønsted base to form a cation **4**⁺. Theoretical calculations can be performed to probe these states and assign their absorption wavelengths. Calculations were initially applied to the

Scheme 2. Possible Protonation States of 4 and Structure of 8
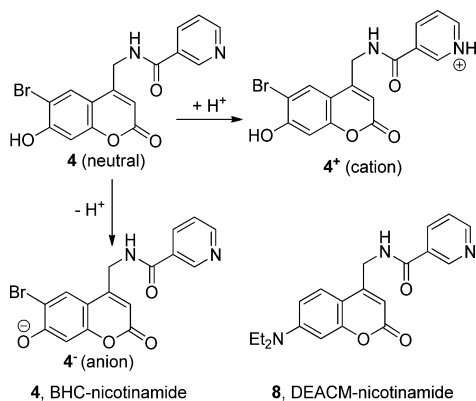
prediction of the UV−vis spectrum values of these three possible protonation states of **4**. DEACM-nicotinamide **8** was also investigated to compare the predicted data for the two systems as shown in Table 2. There are no significant differences for the predicted spectra using the CPCM and

Table 2. Calculated UV−Vis Absorption Wavelength λ_{max} (nm)[a]

		CPCM/M06L/6-311+G**			
entry	structures	H_2O	MeOH	MeCN	DMSO
1	**4**⁻	385	386	386	387
2	**4**	329	329	329	330
3	**4**⁺	332	331	331	333
4	**8**	388	387	387	389
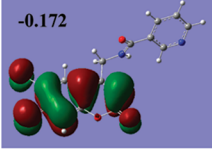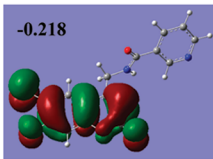
[a].All single point TD-DFT calculations employed in gas-phase optimized structures.
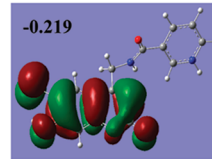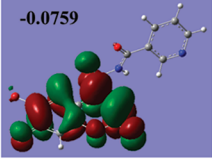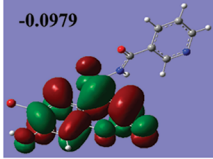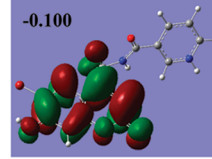
SMD solvation models (for the results using the SMD model, see the Supporting Information). The wavelengths predicted by the CPCM model were slightly higher than that by the SMD model. The UV−vis λ_{max} shown in this paper were calculated using the CPCM model.

As shown in Table 2, the predicted λ_{max} of the cation **4**⁺ and neutral **4** states were similar to each other in all solvents studied. These values all fell within a narrow range of 3 nm centered at about 330 nm. Interestingly, the anion **4**⁻ and neutral **8** have nearly the same λ_{max} values in the range of 385−389 nm without significant solvent effects. These predictions indicated that going from the neutral to the anionic state of BHC-nicotinamide **4** has a much greater impact on the UV−vis spectra than going from the neutral to the cationic state. These predicted results provide a good explanation of the experimentally observed spectra of BHC-nicotinamide **4**, which show a strong red shift from 330 to 370 nm when the pH of solution is increased from 3.06 to 8.07 as shown in Figure 2. The anionic **4**⁻ state dominates in nearly neutral pH conditions. However, further calculations were needed to understand the experimentally observed solvent effect that is not apparent in Table 2.

Despite the difficulties associated with predicting the unexpected solvent effect, the MO pairs responsible for the λ_{max} excitation inspired us to seek an understanding of the predicted spectra. Table 3 summarizes the MO contributions to the UV−vis λ_{max} for each protonation state of complex **4** (for similar MO figures for **8**, see the Supporting Information). All of the MOs shown are localized on the coumarin ring, and the major contributions to the λ_{max} is from the π to the π^* orbital of this ring. The change in protonation state from **4** to **4**⁺ occurs in a different moiety that has no appreciable contribution to the HOMO or LUMO, which is the underlying reason for the smaller change in the HOMO−LUMO gap compared to the change from **4** to **4**⁻ This MO analysis can explain the small solvent effect seen for the protonation of the nicotinamide ring from the neutral **4** to the cationic from **4**⁺. Although the visualized MOs are qualitatively only slightly different for the four structures, their orbital energies are considerably different upon going to the anionic state. For example, the π and π^* orbital energies are −0.218 and −0.0979 (Hartree) for neutral **4** and −0.172 and −0.0759 for anion **4**⁻, respectively. These results show that both the HOMO (π) and LUMO (π^*) energies are increased in the process of the neutral **4** undergoing deprotonation. The HOMO energy (−0.218 to

Table 3. MO Pairs Responsible for the λ_{max} Excitation for Each Charge State (Hartree)[a]

structures	4^-	4	4^+
Occupied MO(s)	−0.172	−0.218	−0.219
Virtual MO(s)	−0.0759	−0.0979	−0.100

[a]All orbitals are taken from CPCM/M06L/6-311+G** single point calculations in water solvent. Isovalue for surface = 0.02.
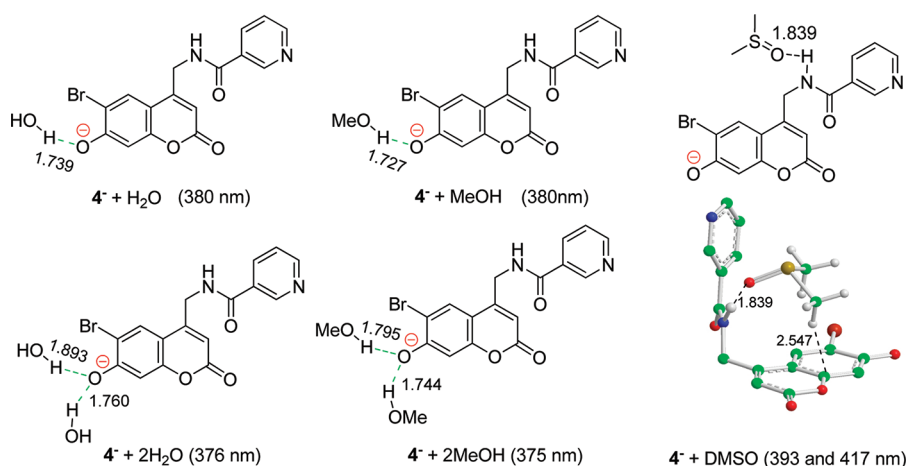

Figure 4. Proposed solvent interactions (bond lengths in Å). All models are based on single-point TD-DFT calculations on each solvent-phase optimized structure.

−0.172 hartree) increased more than the LUMO energy (−0.0979 to −0.0759 hartree), which decreased the gap between this MO pair (0.120 to 0.0961 hartree). These results provide a rational explanation for the greater influence of the transformation of the coumarin rings from the neutral form **4** to the anionic form 4^-.

On the basis of our MO analysis above, we are able to propose molecular models for possible solvent interactions. Special attention was obviously given to hydrogen bond interactions of substituents on the coumarin ring in the protic solvents that were employed in this study. Anion 4^- can form hydrogen bonds with water and methanol as shown in Figure 4. The predicted λ_{max} values tend to undergo a blue shift with an increasing number of hydrogen bonds, because the hydrogen bonds stabilize the HOMO and increase the gap between the HOMO and LUMO. This result can also be inferred from Table 3 for which the HOMO of 4^- has greater charge located on the oxygen compared to the LUMO. Consequently, the H bonding should stabilize the HOMO to a greater extent than the LUMO, thus increasing the energy gap. In the aprotic solvents acetonitrile and DMSO, partial proton dissociation from neutral **4** may occur, which may be an explanation of an extra peak observed at ca. 330 nm in the experimental UV−vis spectrum (Figure 3). Although, there is a weaker hydrogen bond between anion 4^- and DMSO, a large change in the conformation of anion 4^- is induced by this interaction, which

explains the predicted λ_{max} red-shift (Figure 4). All predicted spectra of these models are closely aligned with the experimental observations and provide a rational explanation for the solvent effects observed for BHC-nicotinamide **4**.

Photochemical Characterization. We next investigated the photochemical behavior of the C−N bonded coumarin-labeled nicotinamide derivatives **4** and compared it to the C−O bonded ester derivative **9**, which undergoes cleavage upon irradiation at 369 nm with a quantum yield of 0.036.[23] In stark contrast, the BHC-nicotinamide **4** is stable upon continuous irradiation at 406 nm in DMSO. A possible reason is that the amide bond of BHC-nicotinamide **4** is too stable to undergo cleavage under the photolysis conditions, while BHC-acetate **9** with a relatively weak ester bond is a more suitable cleavage substrate. This conclusion is supported by the energies of the appropriate C−N and C−O σ^* bonds obtained by NBO calculations summarized in Figure 5a. The energy of the antibonding σ^* orbital is higher in **4** (0.323) than in **9** (0.230), which indicates that the C−N bond in compound **4** is less susceptible to cleavage than the C−O bond in compound **9**. These results show that the amide derivatives developed in this study may serve as photostable labeling agents for cellular studies, whereas the more labile ester derivatives functions are already established as useful photocage agents for controlled release of biochemical intermediates.
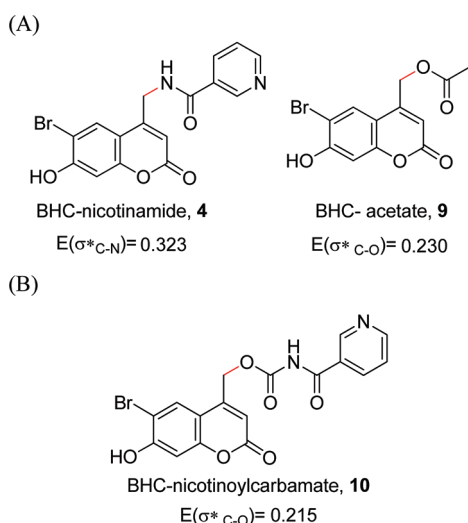
(A)

BHC-nicotinamide, **4**

E(σ*$_{C-N}$)= 0.323

BHC- acetate, **9**

E(σ* $_{C-O}$)= 0.230

(B)

BHC-nicotinoylcarbamate, **10**

E(σ* $_{C-O}$)= 0.215

Figure 5. Energies of natural antibond orbital (Hartree).

■ CONCLUSION AND OUTLOOK

BHC-nicotinamide (**4**) and DEACM-nicotinamide (**8**) have been synthesized, and upon study of solvent effects on the UV−vis absorption of BHC-nicotinamide, we found an unusual photophysical behavior. As the polarity of the solvent increases, a hypsochromic shift was observed in the case for **4**, which is opposite from the usual bathochromic shift. The experimental results were rationalized by predicting the λ_{max} using TD-DFT calculations with the CPCM solvation model. Based on MO analysis, different molecular models were also proposed for possible solvent interactions. Based on NBO analysis, we can suggest future studies of compounds such as BHC-nicotinoylcarbamate **10**[24] (Figure 5B), which may be expected to have photochemical properties that are intermediate between those of photolabile esters such as **9** and the photostable amides such as BHC-nicotinamide **4** in this paper. In preliminary studies, the carbamate C−O σ* bond energy of compound **10** is calculated to be 0.215 hartree, which is close to the value of 0.230 hartree for compound **9**. Using NBO and TD-DFT calculations, we anticipate the possibility of designing related compounds with appropriately tuned wavelengths that may function as desired as either photostable labeling agents or as photolabile cage compounds for cellular studies.

■ EXPERIMENTAL SECTION

General Methods. All experiments were done in the air unless otherwise stated. NMR chemical shifts are given in ppm relative to residual solvent peaks: ¹H (7.27 for CDCl₃ and 2.5 ppm for DMSO-d_6) and ¹³C (77.23 for CDCl₃ and 39.51 ppm for DMSO-d_6). Flash chromatography was performed using 60 Å silica gel.

Synthesis. *6-Bromo-4-(chloromethyl)-7-hydroxy-2H-chromen-2-one (2).* 4-Bromoresorcinol (**1**) (5 g, 26.4 mmol) and ethyl-4-chloroacetoacetate (5.36 mL, 39.7 mmol) were added to methanesulfonic acid (40 mL) and stirred at 25 °C for 2 h. Then ice and water were added, the suspension was filtered, and the solid was dried to obtain 7.63 g (quantitative) of **2** as a beige solid. ¹H NMR (300 MHz, DMSO-d_6) δ 11.59 (brs, 1H), 7.99 (s, 1H), 6.91 (s, 1H), 6.47 (s, 1H), 4.99 (s, 2H) (lit. ¹H NMR).[18]

4-(Aminomethyl)-6-bromo-7-hydroxy-2H-chromen-2-one (3). 6-Bromo-4-(chloromethyl)-7-hydroxy-2H-chromen-2-one (**2**) (2 g, 6.9 mmol) was suspended in aq ammonium hydroxide (70 mL). The solution was degassed, and stirred under nitrogen at 50 °C for 1 h. The

reaction was quenched with 6 N aq HCl, and the precipitate was filtered. The solid was triturated in water to yield 1.1927 g (64% yield) of **3** as an off white solid. IR (KBr) ν_{max} 3230, 3024, 2940, 2669, 1721, 1681, 1591, 1353 cm⁻¹. ¹H NMR (300 MHz, DMSO-d_6) δ 8.58 (brs, 2H), 8.00 (s, 1H), 6.98 (s, 1H), 6.35 (s, 1H), 4.35 (s, 2H). ¹³C NMR (75 MHz, DMSO-d_6) δ 159.2, 157.7, 153.5, 148.0, 128.7, 110.5, 110.3, 106.3, 103.1, 37.9. HRMS calcd for $C_{10}H_9BrNO_3$ 269.9613, found 269.9760.

N-[(6-Bromo-7-hydroxy-2-oxo-2H-chromen-4-yl)methyl]-nicotinamide, BHC-nicotinamide (4). In a flame-dried flask, **3** (200 mg, 0.65 mmol), nicotinoyl chloride hydrochloride (174 mg, 0.975 mmol), and N,N-diisopropylethylamine (0.62 mL, 2.92 mmol) were added to anhydrous dimethylformamide (6 mL). After the mixture was stirred for 2 h, a satd aq sodium bicarbonate was added. The solution was then evaporated under vacuum, and the resulting solid was triturated with water. The suspension was filtered to obtain 183 mg (50% yield) of **4** as beige solid. IR (KBr) ν_{max} 3545, 3315, 3095, 1693, 1658, 1587, 1408 cm⁻¹. ¹H NMR (600 MHz, DMSO-d_6) δ 9.23 (t, J = 5.4 Hz, 2H), 9.07 (dd, J = 0.6 Hz, J = 2.4 Hz, 1H), 8.73 (dd, J = 1.8 Hz, J = 4.8 Hz, 1H), 8.26 (m, 1H), 7.64 (s, 1H), 7.54 (m, 1H), 5.94 (s, 1H), 5.45 (s, 1H), 4.51 (d, J = 6.0 Hz, 2H). ¹³C NMR (150 MHz, DMSO-d_6) δ 170.7, 165.4, 162.3, 157.2, 153.1, 152.5, 148.9, 135.5, 129.9, 126.2, 124.0, 115.8, 103.6, 102.3, 99.3, 39.7. HRMS calcd for $C_{16}H_{12}BrN_2O_4$ 418.9614, found 418.9619. Mp > 230 °C

7-(Diethylamino)-4-(hydroxymethyl)-2H-chromen-2-one (6). In a flame-dried flask, 7-dimethylamino-4-methylcoumarin (**5**) (570 mg, 2.46 mmol) and selenium dioxide (414 mg, 3.73 mmol) were placed in freshly distilled xylene (100 mL). The solution was heated at reflux for 24 h, during which the solution turned dark red. The solution was cooled to 25 °C, filtered through a pad of Celite, and evaporated. Ethanol (100 mL) and sodium borohydride (46 mg, 1.23 mmol) were added to the flask, and the mixture stirred for 4 h. After the solution was neutralized with 1 N HCl, the solution was extracted three times with DCM, dried over magnesium sulfate, and evaporated under vacuum. The residue was purified by flash chromatography (DCM/acetone 5/1) affording 240 mg (39% yield) of **6** as an orange solid. ¹H NMR (300 MHz, CDCl₃). δ 7.32 (d, J = 9.2 Hz, 1H), 6.57 (d, J = 9.2 Hz, 1H), 6.50 (d, J = 2.4 Hz, 1H), 6.27 (s, 1H), 4.84 (s, 2H), 3.40 (q, J = 7.2 Hz, 4H), 2.39 (s, 1H), 1.20 (t, J = 6.8 Hz, 6H) (lit. ¹H NMR).[20]

4-(Chloromethyl)-7-(diethylamino)-2H-chromen-2-one (7). **6** (100 mg, 0.404 mmol), p-toluenesulfonyl chloride (100 mg, 0.526 mmol), pyridine (97 μL, 1.21 mmol) and dry DCM (5 mL) were placed in a round-bottom flask and stirred at 25 °C for 48 h under argon atmosphere. Water was added, and the mixture was extracted three times with DCM, and the combined organic extracts were dried over magnesium sulfate and evaporated. The residue was purified by flash chromatography (pet ether/acetone 15/1) affording 25 mg (24% yield) of 7 as an orange solid. ¹H NMR (300 MHz, CDCl₃) δ 7.45 (d, J = 9.2 Hz, 1H), 6.63 (dd, J = 2.4 Hz, 9.2 Hz, 1H), 6.53 (d, J = 2.4 Hz, 1H), 6.19 (s, 1H), 4.58 (s, 2H), 3.42 (q, J = 7.2 Hz, 4H), 1.21 (t, J = 7.2 Hz, 6H) (lit. ¹H NMR).[20]

N-((7-(Diethylamino)-2-oxo-2H-chromen-4-yl)methyl)-nicotinamide, DEACM-nicotinamide (8). **7** (50 mg, 0.188 mmol) and sodium azide (14 mg, 0.216 mmol) were placed in a flask with dry DMF (1 mL) and stirred at 25 °C for 1 h. Water was added, the mixture was extracted three times with Et₂O, and the combined organic extracts were dried over magnesium sulfate and evaporated. The residue was dissolved in methanol (1 mL) and palladium on carbon (5 mg) was added. The mixture was stirred overnight under hydrogen and filtered through Celite. The solvent was evaporated to give 38 mg of 4-(aminomethyl)-7-(diethylamino)-2H-chromen-2-one as an orange solid. This solid was suspended in dry DMF (1 mL) with nicotinoyl chloride (42 mg, 0.23 mmol) and DIEA (170 μL, 1.03 mmol), and the mixture was stirred for 3 h. Satd aq sodium bicarbonate was added, and the mixture was extracted three times with ethyl acetate, and the combined organic extracts were dried over magnesium sulfate and evaporated. The residue was triturated with a mixture of ethyl acetate and hexane and filtered to give 48 mg (60% yield) of **8** as a pale-yellow solid. IR (KBr) ν_{max} 2972, 1712, 1602, 1526, 1420 cm⁻¹. ¹H NMR (600 MHz, CDCl₃) δ 9.12 (d, J = 2.4 Hz,

1H), 8.73 (dd, $J = 1.8$ Hz, $J = 4.5$ Hz, 1H), 8.22 (dt, $J = 1.8$ Hz, $J = 7.8$ Hz, 1H), 7.47 (d, $J = 9$ Hz, 1H), 7.40 (dd, $J = 4.8$ Hz, $J = 7.8$ Hz, 1H), 6.58 (dd, $J = 2.4$ Hz, $J = 9$ Hz, 1H), 6.42 (d, $J = 2.4$ Hz, 1H), 6.01 (s, 1H), 4.77 (d, $J = 5.4$ Hz, 2H), 3.39 (q, $J = 7.2$ Hz, 4H), 1.20 (t, $J = 7.2$ Hz, 6H). ^{13}C NMR (150 MHz, $CDCl_3$) δ 165.6, 162.4, 156.3, 152.4, 152.2, 150.8, 148.3, 135.3, 125.0, 123.5, 108.9, 106.7, 97.6, 44.7, 40.1, 12.4. HRMS calcd for $C_{20}H_{22}N_3O_3$ 352.1656, found 352.1643. Mp: 95 °C (dec.).

UV–Vis Spectra. UV–vis spectra were recorded in different solvents at a concentration of 50 nM of BHC-nicotinamide or DEACM-nicotinamide. Stock solutions of BHC-nicotinamide at different pH's (3.06−8.07) were made in a 100 mM citrate-phosphate buffer, and UV–vis spectra were recorded immediately. Absorption spectra were corrected for baseline and dilution.

Computational Methods. All structures were optimized in the gas phase with the 6-311+G(d,p) basis set[25,26] under the M06-L[27] level theory of M06 suite functional. No constraints were imposed in the geometry optimizations. To obtain the calculated λ_{max} values, single-point calculations with time dependent density functional theory (TD-DFT)[28−32] were performed on the optimized structures with the same basis set. The TD-DFT calculations were carried out in both the gas-phase and the solvent-phase to evaluate the description of the solvent effect on the calculated spectra. Both the conductor-like polarizable continuum model (CPCM)[33,34] and SMD[35] solvent models were employed within the TD-DFT calculations. The explicit models in Figure 4 are based on single-point TD-DFT calculations on each solvent-phase optimized structure. Natural bond orbital (NBO) analysis was employed. The molecular orbitals (MO) were visualized by Gaussview 5.08. All calculations were done within the Gaussian 09 program.[36]

■ ASSOCIATED CONTENT

Ⓢ Supporting Information

Copies of ^1H and ^{13}C NMR spectra for all the new compounds, geometries and energies from the CPCM and SMD solvation model calculations, structural and photophysical characterization of compounds. This material is available free of charge via the Internet at http://pubs.acs.org.

■ AUTHOR INFORMATION

Corresponding Author

*E-mail: phelquis@nd.edu; owiest@nd.edu.

Author Contributions

Pauline Bourbon and Qian Peng contributed equally to this paper.

Notes

The authors declare no competing financial interest.

■ ACKNOWLEDGMENTS

■ REFERENCES

(1) Wood, P. D.; Johnston, L. J. *J. Phys. Chem. A.* **1998**, *102*, 5585−5591.

(2) Schmidt, R.; Geissler, D.; Hagen, V.; Bendig, J. *J. Phys. Chem. A.* **2007**, *111*, 5768−5774.

(3) Becker, R. S.; Chakravorti, S.; Gartner, C. A.; de Grace Miguel, M. *J. Chem. Soc., Faraday Trans.* **1993**, *89*, 1007−1019.

(4) Rechthaler, K.; Kohler, G. *Chem. Phys.* **1994**, *189*, 99−116.

(5) Henry, B.; Lawler, E. *J. Mol. Spectrosc.* **1973**, *48*, 117−123.

(6) Eckardt, T.; Hagen, V.; Schmidt, R.; Schweitzer, C.; Bendig, J. *J. Org. Chem.* **2002**, 703−710.

(7) Furuta, T.; Wang, S. S.-H.; Dantzker, J. L.; Dore, T. M.; Bybee, W. J.; Callaway, E. M.; Denk, W.; Tsien, R. Y. *Proc. Natl. Acad. Sci. U.S.A.* **1999**, *96*, 1193−1200.

(8) Reichardt, C. *Solvents and Solvent Effects in Organic Chemistry*; VCH: New York, 1991.

(9) Zakerhamidi, M. S.; Ghanadzadeh, A.; Tajalli, H.; Moghadam, M.; Jassas, M.; Hosseini, R. *Spectrochim. Acta, Part A* **2010**, *77*, 337−341.

(10) Aono, S.; Minezawa, N.; Kato, S. *Chem. Phys. Lett.* **2010**, *492*, 193−197.

(11) Kumar, S.; Rao, V. C.; Rastogi, R. C. *Spectrochim. Acta, Part A* **2001**, *57*, 41−47.

(12) Ellis-davies, G. C. R. *Nat. Methods* **2007**, *4*, 619−628.

(13) Lee, H.-M.; Larson, D. R.; Lawrence, D. S. *ACS Chem. Biol.* **2009**, *4*, 409−427.

(14) Mayer, G.; Heckel, A. *Angew. Chem., Int. Ed.* **2006**, *45*, 4900−4921.

(15) Pelliccioli, A. P.; Wirz, J. *Photochem. Photobiol. Sci.* **2002**, *1*, 441−458.

(16) Ando, H.; Furuta, T.; Tsien, R. Y.; Okamoto, H. *Nat. Genet.* **2001**, *28*, 317−325.

(17) Lin, W.; Lawrence, D. S. *J. Org. Chem.* **2002**, *67*, 2723−2726.

(18) Hagen, V.; Kilic, F.; Schaal, J.; Dekowski, B.; Schmidt, R.; Kotzur, N. *J. Org. Chem.* **2010**, *75*, 2790−2797.

(19) Suzuki, A. Z.; Watanabe, T.; Kawamoto, M.; Nishiyama, K.; Yamashita, H.; Ishii, M.; Iwamura, M.; Furuta, T. *Org. Lett.* **2003**, *5*, 4867−4870.

(20) Lin, W.; Long, L.; Tan, W.; Chen, B.; Yuan, L. *Chem.—Eur. J.* **2010**, *16*, 3914−3917.

(21) Lee, M.; Gubernator, N. G.; Sulzer, D.; Sames, D. *J. Am. Chem. Soc.* **2010**, *132*, 8828−8830.

(22) Wolfbeis, O. S.; Marhold, H. *Z. Anal. Chem.* **1987**, *327*, 347−350.

(23) Fedoryak, O. D.; Dore, T. M. *Org. Lett.* **2002**, *4*, 3419−3422.

(24) Our preliminary experimental results show that the analogous DEACM nicotinoyl carbamate undergoes cleavage upon continuous photolysis at 379 nm.

(25) Hariharam, P. C.; Pople, J. A. *Theor. Chim. Acta* **1973**, *28*, 213−222.

(26) Krishnan, R.; Binkley, J. S.; Seeger, R.; Pople, J. A. *J. Chem. Phys.* **1980**, *72*, 650−654.

(27) Zhao, Y.; Truhlar, D. G. *J. Chem. Phys.* **2006**, *125*, 194101−194118.

(28) Runge, E.; Gross, E. K. U. *Phys. Rev. Lett.* **1984**, *52*, 997−1000.

(29) Stratmann, R. E.; Scuseria, G. E.; Frisch, M. J. *J. Chem. Phys.* **1998**, *109*, 8218−8224.

(30) Casida, M. E.; Jamorski, C.; Casida, K. C.; Salahub, D. R. *J. Chem. Phys.* **1998**, *108*, 4439−4449.

(31) Marques, M. A. L.; Gross, E. K. U. *Annu. Rev. Phys. Chem.* **2004**, *55*, 427−455.

(32) Bauernschmitt, R.; Ahlrichs, R. *Chem. Phys. Lett.* **1996**, *256*, 454−464.

(33) Barone, V.; Cossi, M. *J. Phys. Chem.* **1998**, *102*, 1995−2001.

(34) Cossi, M.; Rega, N.; Scalmani, G.; Barone, V. *J. Comput. Chem.* **2003**, *24*, 669−681.

(35) Marenich, A. V.; Cramer, C. J.; Truhlar, D. G. *J. Phys. Chem. B.* **2009**, *113*, 6378−6396.

(36) Frisch, M. J.; Trucks, G. W.; Schlegel, H. B.; Scuseria, G. E.; Robb, M. A.; Cheeseman, J. R.; Scalmani, G.; Barone, V.; Mennucci, B.; Petersson, G. A.; Nakatsuji, H.; Caricato, M.; Li, X.; Hratchian, H. P.; Izmaylov, A. F.; Bloino, J.; Zheng, G.; Sonnenberg, J. L.; Hada, M.;

Ehara, M.; Toyota, K.; Fukuda, R.; Hasegawa, J.; Ishida, M.; Nakajima, T.; Honda, Y.; Kitao, O.; Nakai, H.; Vreven, T.; Montgomery, J. A. J.; Peralta, J. E.; Ogliaro, F.; Bearpark, M.; Heyd, J. J.; Brothers, E.; Kudin, K. N.; Staroverov, V. N.; Kobayashi, R.; Normand, J.; Raghavachari, K.; Rendell, A.; Burant, J. C.; Iyengar, S. S.; Tomasi, J.; Cossi, M.; Rega, N.; Millam, J. M.; Klene, M.; Knox, J. E.; Cross, J. B.; Bakken, V.; Adamo, C.; Jaramillo, J.; Gomperts, R.; Stratmann, R. E.; Yazyev, O.; Austin, A. J.; Cammi, R.; Pomelli, C.; Ochterski, J. W.; Martin, R. L.; Morokuma, K.; Zakrzewski, V. G.; Voth, G. A.; Salvador, P.; Dannenberg, J. J.; Dapprich, S.; Daniels, A. D.; Farkas, O.; Foresman, J. B.; Ortiz, J. V.; Cioslowski, J.; Fox, D. J. *Gaussian 09*, Revision A.O2; Gaussian Inc: Wallongford, CT, 2009.